# Performance Comparison of 24S-10P and 24S-14P Field Excitation Flux Switching Machine with Single DC-Coil Polarity

E. Sulaiman[1], M. F. M. Teridi[1], Z. A. Husin[1], M. Z. Ahmad[1] and T. Kosaka[2]
[1]Universiti Tun Hussein Onn Malaysia, Locked Bag 101, Batu Pahat, Johor, 86400 Malaysia
[2]Nagoya Institute of Technology, 466-8555, Nagoya, Japan

***Abstract*- Flux switching machines (FSMs) that consist of all flux sources in the stator have been developed in recent years due to their advantages of single piece and robust rotor structure suitable for various speed applications. They can be categorized into three groups that are permanent magnet (PM) FSM, field excitation (FE) FSM, and hybrid excitation (HE) FSM. Both PMFSM and FEFSM has only PM and field excitation coil (FEC), respectively as their main flux sources, while HEFSM combines both PM and FECs. Among these FSMs, the FEFSM offers advantages of low cost, simple construction and variable flux control capabilities suitable for various performances. In this paper, design study and flux interaction analysis of a new 12S-10P and 12S-14P FEFSM with single direction of DC FEC winding are presented. Initially, design procedures of the FEFSM including parts drawing, materials and conditions setting, and properties setting are explained. Then, coil arrangement tests are examined to confirm the machine operating principle and position of each armature coil phase. Finally, flux interaction between DC FEC and armature coil, FEC flux capabilities at various current condition, induced voltage and initial torque are also analyzed.**

## I. INTRODUCTION

Flux switching machines (FSMs) that consist of all flux sources in the stator have been developed in recent years due to their advantages of single piece and robust rotor structure suitable for various performances and various speed applications. The earliest growth of FSM that is a single-phase 4S-4P permanent magnet (PM) FSM with limited angle actuator or more well-known as Laws relay has been introduced and published in 1952 [1]. Three years later it has been extended to a single-phase generator with 4 stator slots with 4 and 6 rotor poles (4S-4P and 4S-6P) [2]. Over the last ten years, many novel and new FSMs topologies have been developed for various applications, ranging from low cost domestic appliances, automotive, wind power, aerospace, as well as traction drive etc [3-5]. The FSMs can be categorized into three groups that are permanent magnet (PM) FSMs, field excitation (FE) FSMs, and hybrid excitation (HE) FSMs. Both PMFSMs and FEFSMs have only PM and field excitation coil (FEC), respectively as their main flux sources, while HEFSMs combines both PM and FECs in the stator [6-7].

Among several class of FSMs, the FEFSMs offers numerous advantages such as magnet-less machine, low cost, simple construction, and variable flux control capabilities suitable for various performances. The concept of the FEFSMs involves changing the polarity of the DC FEC flux linking with the armature coil flux, with respect to the rotor position. Fig. 1 illustrates four examples of FEFSM available in the literature. To form the FEFSMs, the PM excitation on the stator of conventional PMFSMs is replaced by DC FEC windings for their main flux sources. In other words, the FEFSMs are a structure of salient rotor reluctance machine with a novel topology, combining the principles of induction generator and switch reluctance machine [8-9].

Early examples of single-phase 4S-2P FEFSM that employs a DC FEC as their main flux sources, a toothed-rotor structure and fully-pitched windings on the stator is shown in Fig. 1(a) [10]. It is obvious that both armature coil and DC FEC windings are placed in the stator which overlapped each other. The practicality of this design has been demonstrated in

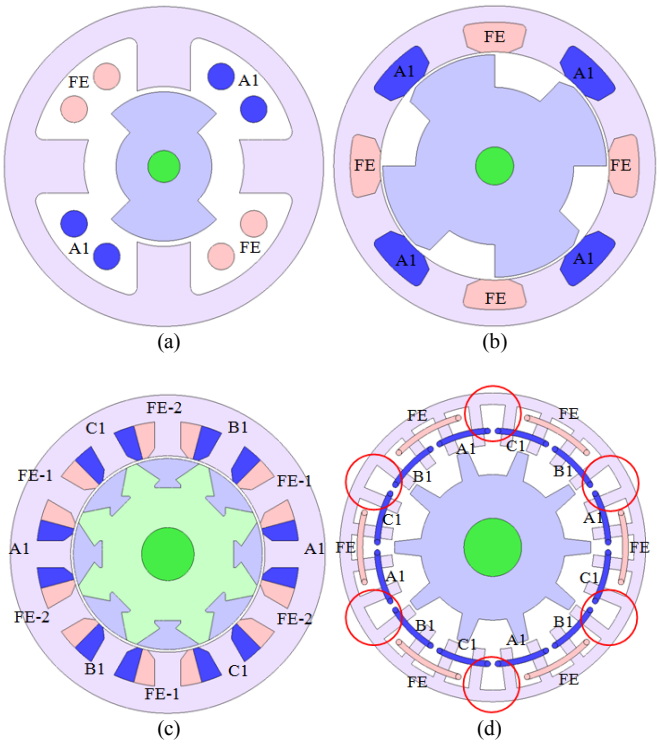


Fig. 1. Examples of FEFSMs (a) 1-phase 4S-2P (b) 1-phase 8S-4P (c) 3-phase 12S-8P with segmented rotor (d) 3-phase 24S-10P

978-1-4673-5074-7/13/$31.00 ©2013 IEEE

various applications requiring high power densities with a good level of durability [11-12]. The originality of the machine is that a single-phase ac waveform could be realized in the armature windings by deployment of DC FEC. Consequently, with armature coil flux interaction in zero rotor position, the maximum flux orientation required for rotor rotation is generated. Hence, the torque is produced by the variable mutual inductance of the windings. Although the single-phase FEFSM can be consider as a very simple machine to manufacture, it requires two power electronic controllers for armature coil and DC FEC. Thus it has the potential to be extremely low cost only in high volume applications. Furthermore, being an electronically commutated brushless machine, FEFSM inherently offers longer life, and very flexible and precise control of torque, speed, and position at no additional cost.

Another example of single-phase FEFSM is depicted in Fig. 1(b) with eight stator slots and four rotor poles (8S-4P) [13]. From the figure, the DC FEC windings in four of the slots are fed with direct current to establish four pole magnetic fields. The orher four slots contain an armature winding that also pitched over two stator teeth. The direction of the current in the armature winding determines a set of four stator poles carries flux and also the position of the rotor. Since the DC FEC is excited by unipolar current, it can be directly connected in parallel or in series with the dc-supply of power converter which feeds the bipolar current into the armature winding. The design principle is explained in [14], and the single-phase 8S-4P FEFSM has achieved higher output power density and much higher efficiency when compared with the induction machine (IM). However, the single-phase FEFSMs suffer with problems of low starting torque, large torque ripple, fixed rotating direction, and overlapped windings between armature coil and DC FEC.

To improve the drawbacks of FEFSMs, a three-phase 12S-8P with segmental rotor and 24S-10P FEFSMs have been developed as shown in Figs. 1(c) and (d), respectively. For 12S-8P FEFSM, segmental rotor is used to provide a clear magnetic path for conveying the field flux to adjacent stator armature coil following the rotor rotation. This design gives shorter end windings of totally separated DC FEC and armature coil when compared with the toothed-rotor structure which is associated with overlapping coils. There are significant gains with this arrangement as it uses less conductor materials, thus the overall machine efficiency can be improved due to reduction of copper loss [15].

Furthermore, Fig. 1(d) illustrates the 24S-10P FEFSM which is redesigned from the 24S-10P PMFSM. In this structure, the PM is removed from the stator and half of the armature coil slots in the upper layer of PMFSM are placed with the DC FEC windings [16]. Since the adjacent DC FECs are isolated as shown in red circle in Fig. 1(d), the total flux generation is limited and thus reducing the performances.

In this paper, a new structure of 24S-10P and 24S-14P FEFSMs with single DC FEC polarity are proposed and compared. In contrast with alternate flux polarities from adjacent DC FEC of 24S-10P FEFSM mentioned above, the DC FEC of the proposed FEFSMs is arranged with a single polarity of DC current source. The advantages of the proposed machines are easy manufacturing of single DC FEC windings, low copper loss due to less volume of FEC, less flux leakage when compared with dual FEC adjacent windings, and design freedom of FEC for various performances.

## II. Design Methodology of The Proposed FEFSM

In this paper, design study and performance analysis of the 24S-10P and 24S-14P FEFSMs are investigated. The initial FEFSMs configurations and dimensions are illustrated in Fig. 2 and Table I, respectively. From the structure, it is clear that the FEFSMs is having 24 stator teeth, 10/14 rotor poles, and alternate DC FEC and armature coil slot around the stator. The DC FEC is wound in counter-clockwise polarity, while the three-phase armature coils are placed in between them.

Commercial FEA package, JMAG-Designer ver.12.0, released by Japan Research Institute (JRI) is used as 2D-FEA solver for this design. Firstly, JMAG Editor is used to draw the rotor, stator, armature coil and DC FEC. Then, the materials, conditions, circuits and properties of the machine are set in JMAG Designer. The design process of part drawing and condition setting are demonstrated in Fig. 3. Furthermore, coil

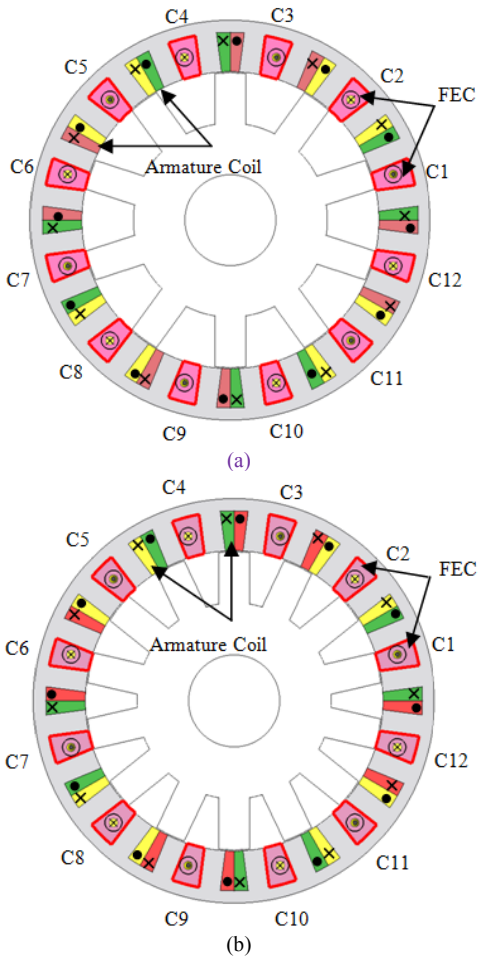


Fig. 2. Initial design of FEFSMs (a) 24S-10P (b) 24S-14P

TABLE I. PARAMETERS SPECIFICATIONS OF THE INITIAL 24S-10P AND 24S-14P FEFSMS

| Parameters | 24S-10P | 24S-14P |
|---|---|---|
| Number of phase | 3 | 3 |
| Number of stator poles | 12 | 12 |
| Number of rotor poles | 10 | 14 |
| Outer radius of stator | 132mm | 132mm |
| Stack length | 70mm | 70mm |
| Air gap length | 0.8mm | 0.8mm |
| Inner radius of stator | 97.2mm | 97.2mm |
| Stator tooth top width | 14mm | 14mm |
| Stator tooth bottom width | 14mm | 14mm |
| Stator yoke thickness | 8mm | 8mm |
| Rotor tooth width | 20mm | 20mm |
| Number of phase turns | 8 | 8 |
| Number of DC winding turns | 60 | 60 |

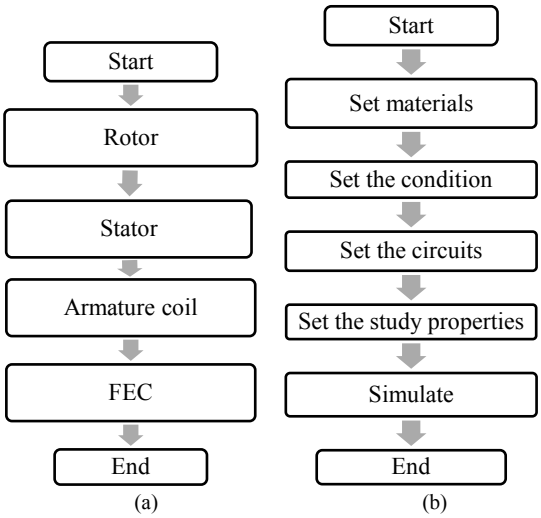


Fig. 3: Design methodology of the proposed FEFSMs
(a) Parts drawing (b) Conditions setting

arrangement tests are examined to validate the operating principle of both FEFSMs and to set the position of each armature coil phase. Then, the flux linkage at various DC FEC current densities, $J_E$ flux linkages, flux distributions at zero rotor position, and induced voltage are compared. Finally, the torque at various DC FEC current densities, $J_E$ of both FEFSMs is also analyzed.

## III. PERFORMANCE OF THE PROPOSED FEFSMS BASED ON 2D-FEA

### A. *Armature Coil Arrangement Test*

In order to validate the operating principle of the FEFSMs and to set the position of each armature coil phase, coil arrangement tests are examined in all 12 armature coils separately. Initially, all armature coil and DC FEC are wounded in counter-clockwise direction. Then, a dc current is supplied to the DC FEC windings at current density, $J_E$ of $30A/mm^2$ and the flux linkage at each armature coil is observed. The resulting flux linkages at each armature coil are compared and the three phase armature coil is defined according to the conventional 120° phase shifted between all phases. Figs. 4 and 5 illustrate the three-phase flux linkage of 24S-10P and 24S-14P FEFSMs defined as U, V, and W, respectively. It is obvious that all flux linkages produce are purely sinusoidal with maximum flux of 0.0430Wb and 0.0361Wb for 24S-10P and 24S-14P FEFSMs, respectively. Thus, the coil tests to proof the principles and to get three phase flux linkages of the FEFSMs are successfully achieved.

### B. *DC FEC Flux Characteristics at Various DC FEC Current Densities, $J_E$*

The DC FEC flux characteristics at various DC FEC current densities, $J_E$ for 24S-10P and 24S-14P are also investigated as illustrated in Fig. 6 to 8, respectively. From the figures, it is clear that initially the flux pattern is increased with the increase in current density until DC FEC current density, $J_E$ of $15A/mm^2$. However, the flux generated starts to reduce when higher DC FEC current density is injected to the system as demonstrated in Fig. 8. It is expected that this phenomena occurs due to some flux leakage and flux cancellation that will be investigated in future. In addition, although the flux generated from 24S-14P design is slightly less than 24S-10P FEFSM, it obvious that 24S-14P design has additional four poles more than 10 poles rotor. With similar width of rotor pole at initial design, the 14 poles rotor has much larger area and thus the flux flows become more distributed when compared with 10 poles rotor. The flux lines and flux distribution at zero rotor position of DC FEC for both 24S-10P and 24S-14P FEFSMs are illustrated in Figs. 9 and 10, respectively. It is clear that all flux lines flow from stator to rotor and return

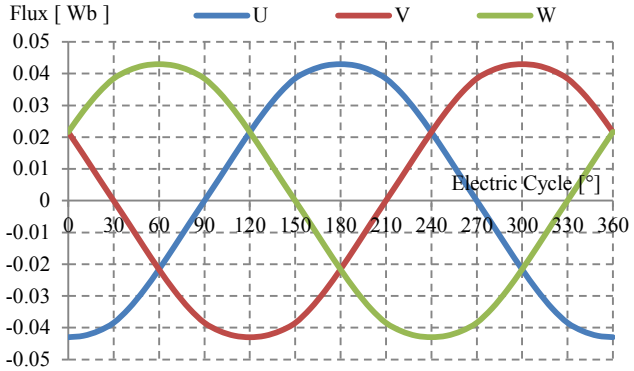


Fig. 4. Three-phase flux linkage of 24S-10P FEFSM

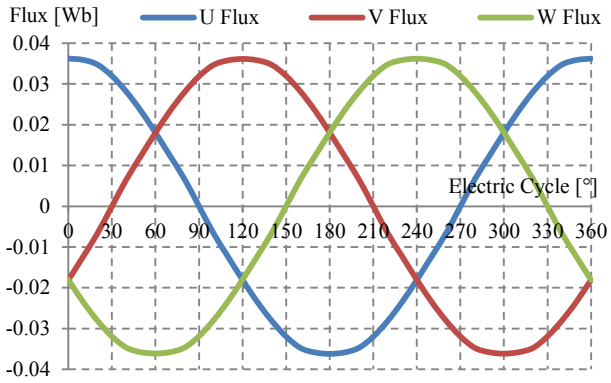


Fig. 5. Three-phase flux linkage of 24S-14P FEFSM

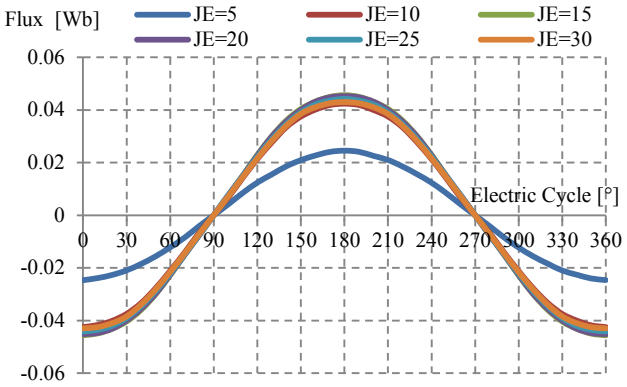


Fig. 6. Flux linkage at various DC FEC current densities, $J_E$ of 24S-10P

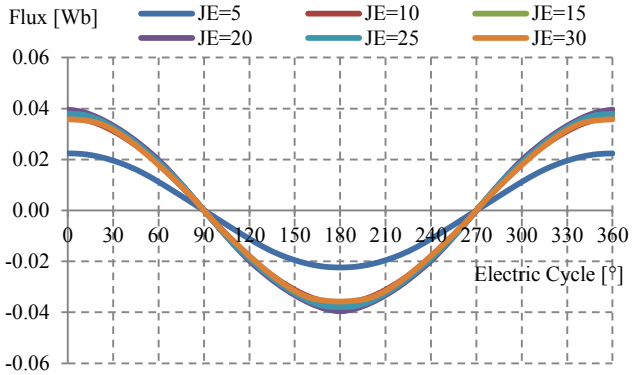


Fig. 7. Flux linkage at various DC FEC current densities, $J_E$ of 24S-14P

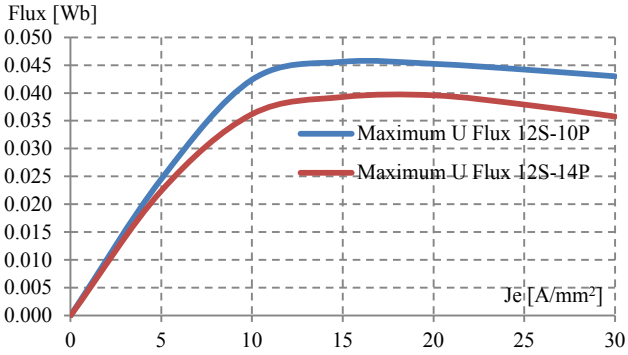


Fig. 8: Maximum flux at various Je for 24S-10PP and 24S-14P FEFSM

through adjacent rotor to make a complete flux cycle. Meanwhile, most of the fluxes are distributed and saturated at rotor air gap and stator outer pitch with magnetic flux density of more than 2 Tesla. From design view point, the rotor air gap can be reduced to decrease the flux leakage, while the stator outer pitch can be increased to reduce the flux saturation.

### *C. Armature Coil vs DC FEC Flux Linkage at Various Current Densities, $J_E$*

The amplitude of armature coil and DC FEC flux linkage at various armature coil and DC FEC current densities, $J_A$ and $J_E$ respectively are compared in Fig. 11. For both FEFSMs, the maximum armature coil flux linkages are more than double when compared with both DC FEC flux linkages. This is due to high ac armature reaction and high flux generated in the

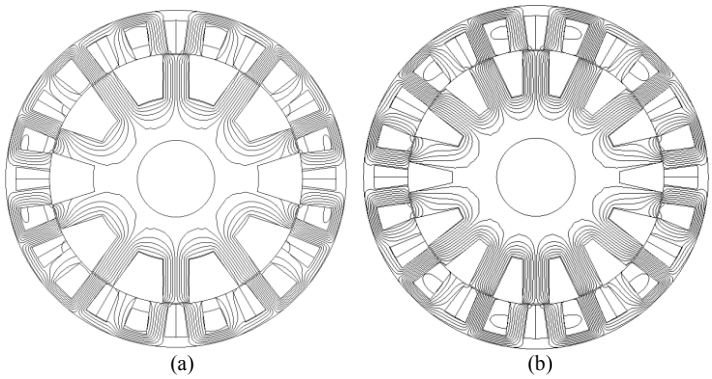


Fig. 9. Flux lines at zero rotor position (a) 24S-10P (b) 24S-14P

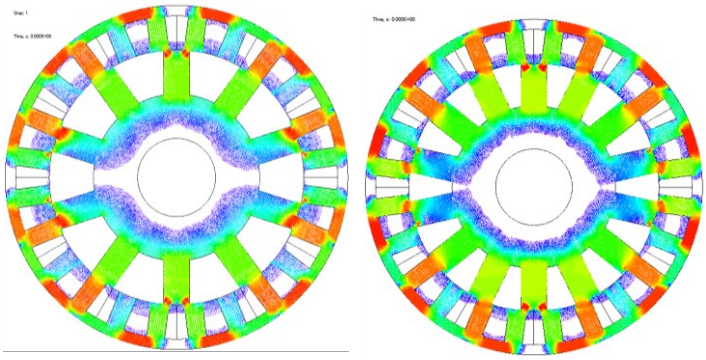


Fig. 10. Flux distribution at zero rotor position (a) 24S-10P (b) 24S-14P

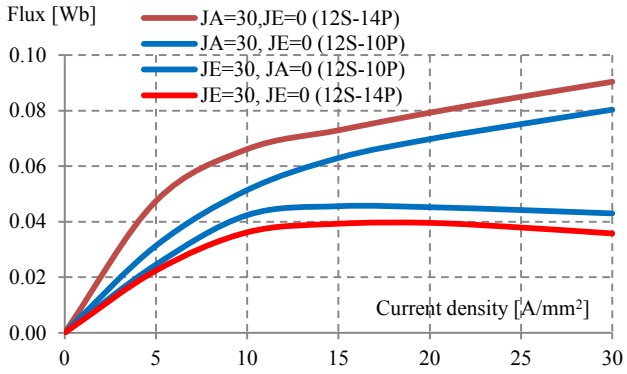


Fig. 11: Comparison of flux generated at various DC FEC and armature coil current density for 24S-10P and 24S-14P FEFSM

armature coil itself. However, in contrast with DC FEC flux linkages, the armature coil flux in 24S-14P is slightly higher than the 24S-10P FEFSM. Thus it is expected that similar performances will be achieved for both FEFSMs due to their balance in flux linkage characteristics. In addition, since the armature flux linkage is generated by armature coil itself, the flux increase linearly with the increase in the current densities.

### *D. Induced Voltage at Open Circuit Condition*

The induced voltage generated from DC FEC flux at open circuit condition of both HEFSMs at various DC FEC current densities, $J_E$ are illustrated in Figs. 12 and 13, respectively. The

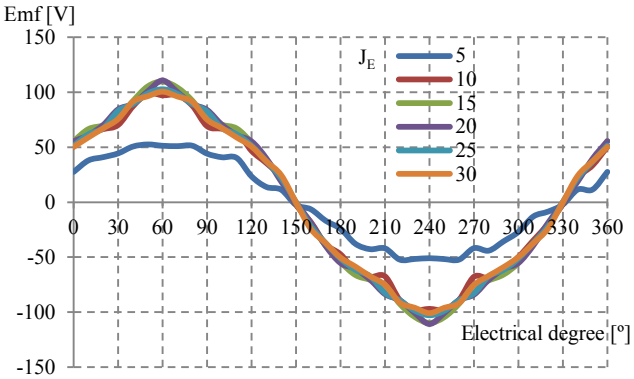


Fig. 12. Induced voltage at various $J_E$ of 24S-10P FEFSM

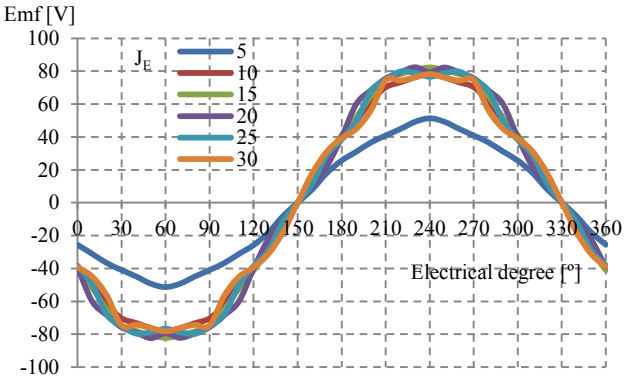


Fig. 13. Induced voltage at various $J_E$ of 24S-14P FEFSM

voltage generated is slightly sinusoidal at low DC FEC current density of 5A/mm$^2$ and becomes more distorted when higher DC FEC current density is introduced. This is due to the third harmonic order from the initial flux itself. The maximum induced voltage generated at maximum DC FEC current density of 30A/mm$^2$ for both 24S-10P and 24S-14P FEFSMs are approximately 110.65V and 82.29V, respectively.

### *E. Torque vs DC FEC Current Density, $J_E$ at Various Armature Current Densities, $J_A$ Characteristics*

The torque versus DC FEC current density, $J_E$ characteristics of 24S-10P and 24S-14P FEFSMs at various armature current densities, $J_A$ are plotted in Figs. 14 and 15, respectively. Form both graphs, the same pattern of linear increment of torque with respect to increase in $J_E$ and $J_A$ is observed.

At low armature coil current density of 5A$_{rms}$/mm$^2$ the torque increased until DC FEC current density of 10A/mm$^2$ and becomes constant when higher DC FEC current density is injected. This is due to low armature coil flux that limits the force to move the rotor. Similarly, the same phenomenon occurs at armature coil current density of 10A$_{rms}$/mm$^2$ and 15A$_{rms}$/mm$^2$, where the torque starts to become constant at DC FEC current density of 15A/mm$^2$ and 20A/mm$^2$, respectively. Therefore, a good balance between DC FEC and armature coil current densities should be determined to get the required torque at specific condition while minimizing the copper loss.

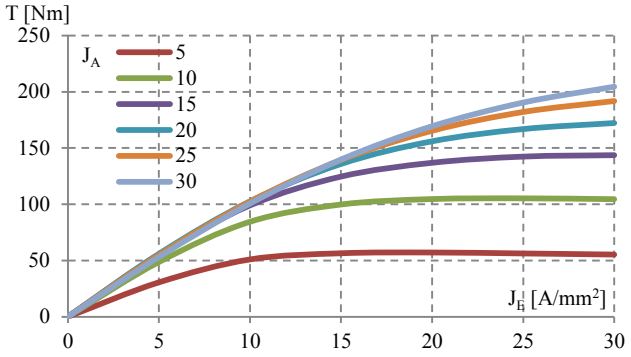


Fig. 14: Torque vs. $J_E$ at various $J_A$ for 24S-10P FEFSM

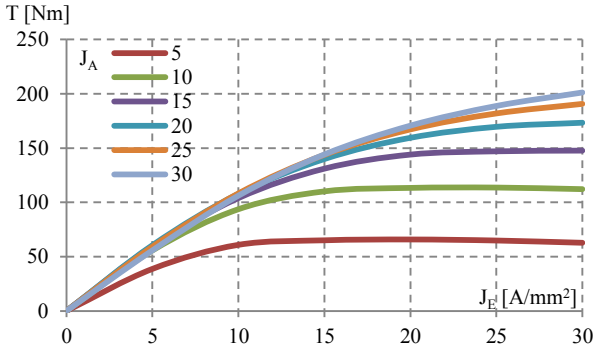


Fig. 15: Torque vs. $J_E$ at various $J_A$ for 24S-14P FEFSM

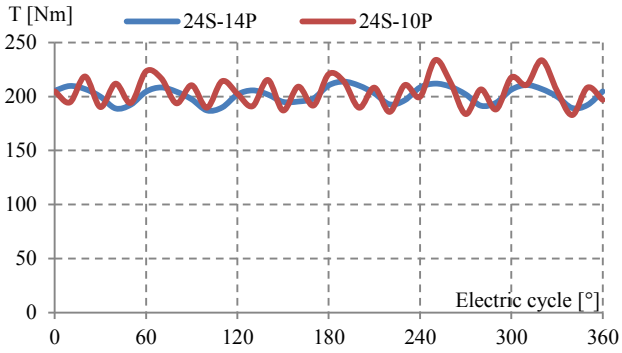


Fig. 16: Instantaneous torque characteristics of both FEFSMs

The maximum torque of 204.5Nm and 201.2Nm are obtained at maximum $J_E$ and $J_A$ of 30A/mm$^2$ and 30A$_{rms}$/mm$^2$, respectively for both FEFSMs, resulting in the corresponding power of 25.7kW and 25.3kW at the speed of 1,200r/min. Since the torque and power generated in 24S-14P FEFSM are slightly less than 24S-10P FEFSM, design improvement and optimization will be conducted in future.

The instantaneous torque characteristics at maximum DC FEC and armature coil current densities of 30A/mm$^2$ and 30A$_{rms}$/mm$^2$ for both 24S-10P and 24S-14P FEFSMs are depicted in Fig. 16. The peak-to-peak torques generated are approximately 26.6Nm and 50.9Nm for both machines.

## IV. CONCLUSION

In this paper, design study and performance comparison of 24S-10P and 24S-14P FEFSMs with single DC FEC polarity have been investigated. The proposed machine has very simple configuration as well as no permanent magnet and thus, it can be expected as very low cost machine. The procedure to design the FEFSMs has been clearly explained. The coil arrangement test has been examined to validate each armature coil phase and to proof the operating principle of the machine. The performances of both FEFSMs such as flux capability and initial torque have been investigated. The machine has the advantages of easy manufacturing, low copper loss due to less FEC, less flux leakage when compared with alternate FEC polarity of adjacent windings, and design freedom of FEC for various performances. Finally, the proposed FEFSM is suitable for various applications with various performances.

## REFERENCES


[1] A.E. Laws: "An electromechanical transducer with permanent magnet polarization," Technical Note No.G.W.202, Royal Aircraft Establishment, Farnborough, UK, 1952.

[2] S. E. Rauch and L. J. Johnson: "Design principles of flux-switching alternators," *AIEE Trans*., vol.74, no.3, pp.1261-1268, Jan 1955.

[3] Y. Amara, E. Hoang, M. Gabsi, and M. Lecrivain: "Design and comparison of different flux-switching synchronous machines for an aircraft oil breather application", Euro. Trans. Electr. Power, no. 15, pp. 497-511, 2005.

[4] W. Hua, M. Cheng, and G. Zhang: "A novel hybrid excitation flux-switching motor for hybrid vehicles", IEEE Trans. Magn., vol. 45, no. 10, pp. 4728-4731, Dec. 2009.

[5] C. Pollock, H. Pollock, R. Barron, J. R. Coles, D. Moule, A. Court, and R. Sutton: "Flux-switching motors for automotive applications", IEEE Trans. Ind. Appl., vol. 42, no. 5, pp. 1177-1184, 2006.

[6] E. Sulaiman, T. Kosaka, and N. Matsui: "High power density design of 6slot-8pole hybrid excitation flux switching machine for hybrid electric vehicles", *IEEE Trans. on Magn.,* vol.47, no.10 pp. 4453-4456, Oct. 2011.

[7] E. Sulaiman, T. Kosaka, and N. Matsui: "Design optimization and performance of a novel 6-slot 5-pole PMFSM with hybrid excitation for hybrid electric vehicle", *IEEJ Trans. Ind. Appl.*, vol.132, no.2, sec.D, pp.211-218, 2012.

[8] J. H. Walker: "The theory of the inductor alternator," *J. IEE*, vol.89, no.9, pp.227–241, June 1942.

[9] T. J. E. Miller: "Switched Reluctance Machines and Their Control", Hillsboro, OH: Magna Physics, 1993.

[10] C. Pollock and M. Wallace: "The flux switching motor, a DC motor without magnets or brushes," *Proc. Conf. Rec. IEEE IAS Annual Meeting*, vol.3, pp.1980–1987, 1999.

[11] H. Pollock, C. Pollock, R. T. Walter, and B. V. Gorti: "Low cost, high power density, flux switching machines and drives for power tools," *Proc. Conf. Rec. IEEE IAS Annual Meeting*, pp.1451–1457, 2003.

[12] C. Pollock, H. Pollock, and M. Brackley: "Electronically controlled flux switching motors: A comparison with an induction motor driving an axial fan", *Proc. Conf. Rec. IEEE IAS Annual Meeting*, pp.2465–2470, 2003.

[13] C. Pollock, H. Pollock, R. Barron, J. R. Coles, D. Moule, A. Court, and R. Sutton: "Flux-switching motors for automotive applications", *IEEE Trans. Ind. Appl*., vol.42, no.5, pp.1177–1184, Sep./Oct. 2006.

[14] J. F. Bangura: "Design of high-power density and relatively high efficiency flux-switching motor", *IEEE Trans. Energy Convers*., vol.21, no.2, pp.416–424, June 2006.

[15] A. Zulu, B. Mecrow, and A. Armstrong: "A wound-field three-phase flux-switching synchronous motor with all excitation sources on the stator", *IEEE Trans. Ind. Appl.*, vol.46, pp.2363-2371, Nov. 2010.

[16] J. T. Chen, Z. Q. Zhu, S. Iwasaki, and R. Deodhar: "Low cost flux-switching brushless AC machines", *Proc. IEEE Vehicle Power and Propulsion Conf*., VPPC 2010, Lille, France, Sept. 2010.